Electronic Supporting Information (ESI)

NZVI Modified Magnetic Filter Paper with High Redox and Catalytic Activities for Advanced Water Treatment Technologies

K. K. R. Datta,[1] E. Petala,[1,2] K. J. Datta,[1] J. A. Perman,[1] J. Tucek,[1] P. Bartak,[3] M. Otyepka,[1] G. Zoppellaro[1,*] and R. Zboril[1,*]

[1] Regional Centre of Advanced Technologies and Materials, Department of Physical Chemistry, Faculty of Science, Palacky University in Olomouc, Slechtitelu 11, 78371 Olomouc, Czech Republic.

[2] Department of Materials Science and Engineering, University of Ioannina, GR-45110 Ioannina, Greece.

[3] Regional Centre of Advanced Technologies and Materials Department of Analytical Chemistry, Faculty of Science, Palacky University in Olomouc, Slechtitelu 11, 78371 Olomouc, Czech Republic.

* Corresponding authors: Phone: +420 585634950, Fax: +420585634761, E-mail address: giorgio.zoppellaro@upol.cz (Giorgio Zoppellaro); Phone: +420 585634337, Fax: +420 585634761, E-mail address: radek.zboril@upol.cz (Radek Zboril).

Number of pages: 16
Number of figures: 10
Number of schemes: 1
Number of tables: 2

Supporting text

Chemicals

All the purchased chemical reagents were used without any further purification. Following chemical were used: Iron (III) chloride hexahydrate ($FeCl_3.6H_2O$), potassium dichromate ($K_2Cr_2O_7$), 1,5-diphenylcarbazide, hydrogen peroxide (H_2O_2) from Sigma-Aldrich, ethanol, acetone analytical grade, sodium borohydride ($NaBH_4$), concentrated phosphoric acid and Phenol from Merck. Filter paper (Grade 40, r = 55 mm) were obtained from Whatman. Trifluoroacetic acid and hexamethyldisilazane as well as standards of phenol, hydroquinone and resorcinol were purchased from Sigma-Aldrich.

Experimental Section

In-situ synthesis of NZVI over FP: The preparation of NZVI embedded in FP consisted of two simple steps, first one involving the impregnation of FP with ferric chloride salt followed by the chemical reduction with $NaBH_4$. In particular, 0.25 g of ferric chloride hexahydrate was dissolved in 2 mL ethanol. FP was impregnated with the metallic solution followed by air-drying, procedure that gave a yellow colored FP. The reducing agent was prepared by dissolving 0.5 g of $NaBH_4$ in 100 mL of deionized water. The Fe^{3+} ions-coated FP was simply dipped in the $NaBH_4$ solution for 45 min, giving rise to a black colored magnetic paper (NZVI@FP). The composite was washed thoroughly with deionized water, then with absolute ethanol and finally dried under vacuum. The amount of NZVI in the FP was found to be ~12 mg (i.e., 5 % of the total weight of the NZVI@FP). Similarly, various loadings of NZVI over FP were prepared by using appropriate amounts of $FeCl_3 \cdot 6H_2O$ and $NaBH_4$ with following proportions, e.g., 0.125 g of ferric chloride hexahydrate and 0.5 g of $NaBH_4$ gave ~2.5 % NZVI loading, 0.2 g of ferric chloride hexahydrate and 0.5 g of $NaBH_4$ gave ~4 % NZVI loading.

Ex-situ synthesis of NZVI over FP: Zero-valent iron nanoparticles (NZVI) were prepared by following the $NaBH_4$ reduction method as reported elsewhere.[1] In particular, 1 g of $FeCl_3 \cdot 6H_2O$ was dissolved in 50 mL of ethanol. The reducing agent was prepared by dissolving 1 g of $NaBH_4$ in 50 mL of deionized water and added drop-wise to the Fe^{3+} solution. The mixture was allowed to settle for 15 min and the particles (recovered via magnet) were washed three times with absolute ethanol and then dried under vacuum. The obtained NZVI powder was stored in an inert

atmosphere prior to the loading on FP. The FP was soaked in 40 mg of NZVI powder in 10 mL of EtOH and the material was sonicated for 15 min, followed by washing with ethanol and drying under vacuum. The amount of NZVI present in the FP was found to be ~8 mg, equal to 3 % of the total weight of the composite.

Determination of hexavalent chromium

UV–Vis spectroscopy was used for the determination of aqueous hexavalent chromium Cr(VI) by the 1,5-diphenylcarbazide method. Dissolved Cr(VI) reacts with diphenylcarbazide in acidic solution to form a red-purple "chromium 1,5-diphenyl-carbohydrazide complex" that shows absorbance maximum at 542 nm. Diphenylcarbazide solution (10 mM) was prepared by dissolving 0.025 g 1,5-diphenylcarbohydrazide in 10 mL acetone. The solution was stored in a closed flask at 4 °C up to 7 days. Phosphoric acid solution was prepared by diluting 0.5 mL concentrated phosphoric acid in 10 mL deionized water. To each tested solution (3 mL) 120 μL of the diphenylcarbazide solution and 60 μL of the phosphoric acid solution were added. The solution was stirred and left for 10 minutes to allow complexation between Cr(VI) and diphenylcarbazide, resulting in a noticeable color change from colorless to violet. The calibration curves were initially determined by using the absorbance spectra of standard chromium solutions.

Remediation of Cr(VI) through filtration

NZVI@FP (5 wt% of NZVI), ex-situ synthesized NZVI deposited over FP (3 wt% of NZVI), neat FP (0 wt% of NZVI) were used as filtration membranes for the remediation of Cr(VI). 30 mL of Cr(VI) solution ($[Cr(VI)]_0$ = 6.5 mg/L) was slowly added through these membranes and the filtrate was collected. For efficient remediation of Cr(VI), the filtrate is again passed through the same membrane. This procedure is repeated for 3 times. The filtrate obtained after 3 cycles was separated and tested by UV-Vis absorption spectroscopy to determine unreduced Cr(VI) by the 1,5-diphenylcarbazide method.

Procedure and assessment of the phenol hydroxylation reaction

The reactions were performed in a conical flask under simultaneous stirring using a hotplate stirrer (Heidolph 3001K). 165 mg of phenol was dissolved in 17 mL deionized water. To this

solution, 0.36 mL of H_2O_2 (30 %) was added (H_2O_2/phenol molar ratio equal to 2:1). This reaction mixture is referred as initial solution and was stirred for 2 min at 40 °C and was allowed to pass through NZVI@FP (5 % of NZVI) supported on Coors™ Buchner funnel. The filtrate was collected and is referred as first filtration. For efficient hydroxylation the filtrate is again passed through the same NZVI@FP membrane three times. This procedure was also tested for neat FP. In all these cases aliquots of 3 mL filtrate was taken immediately using a syringe filter (PTFE, 25 mm, 0.22 μm) and was centrifuged to obtain a clear solution, which was analyzed by GC and GC-MS. Furthermore bare NZVI powder was also tested for its catalytic activity. 12 mg of freshly prepared NZVI (similar amount that is present in NZVI@FP) was added to the initial solution and was allowed to stir for 12 h. A portion of the liquid is taken at regular intervals of time and was centrifuged to obtain a clear solution, which was analyzed by GC and GC-MS.

Characterization techniques

The NZVI@FP (5 wt%) film was sonicated for 2 minutes in ethanol. The obtained dispersion was drop-casted on a carbon-coated copper grid. TEM images were taken employing a JEOL 2010F microscope operated at 200 kV (LaB6 cathode, resolution 0.19 nm) using carbon coated copper grid. Scanning electron microscopy (SEM) images on NZVI@FP were captured on a Hitachi 6600 FEG microscope operating in the secondary electron mode and using an accelerating voltage of 5 kV.

X-ray diffraction (XRD) patterns were recorded on an X'Pert PRO MPD diffractometer (PANalytical, Netherlands) using iron-filtered Co K_α radiation (λ = 0.178901 nm, 40 kV, 30 mA).

Zero-field ^{57}Fe Mössbauer spectrum of the studied sample was recorded at 300 K employing a Mössbauer spectrometer operating at a constant acceleration mode and equipped with a 50 mCi ^{57}Co(Rh) source. The in-field ^{57}Fe Mössbauer spectrum was measured at 5 K by placing the sample into a cryomagnetic system (Oxford Instruments) and exposed to an external magnetic field of 5 T, applied parallel to the direction of γ-rays propagation. The values of the isomer shift are reported with respect to α-Fe.

A superconducting quantum interference device (SQUID, MPMS XL-7, Quantum Design) has been used for the magnetic measurements. The hysteresis loops were collected at a temperature of 5 K and 300 K in external magnetic fields from – 5 T to + 5 T. The zero-field-cooled (ZFC)

and field-cooled (FC) magnetization curves were recorded on warming in the temperature range from 5 to 300 K and in an external magnetic field of 0.01 T after cooling in a zero magnetic field and a field of 0.01 T, respectively.

X-ray photoelectron spectroscopy (XPS) was performed on a PHI 5000 Versa Probe II scanning XPS microprobe from Physical Electronics, using X-ray radiation from an Al source equipped with a monochromator. Samples were in a vacuum of 1.4 x 10^{-7} Pa and presputtered for 30 seconds with argon ions prior to measurement using 50 W, 15 kV power source scanning a 200 micron sample spot at room temperature of 22 °C. Spectra were collected and evaluated with the MultiPak (ULVAC-PHI, Inc.) software. All binding energies were referenced to the C1s peak at 248.8 eV.

The phenol conversion was monitored by a gas chromatograph (GC) Agilent 6820 equipped with capillary column Agilent DB-5 under the operation parameters: Inlet temperature: 300 C, FID temperature: 300 °C, temperature ramp of the oven: 80 °C to 250 °C at a rate of 10 °C/min.

Hydroxylated products were identified by gas chromatography-mass spectrometry (GC-MS). The presence of hydroxyl group(s) was proved by chemical conversion to respective trimethylsilyl ethers performed as follows: 50 μL of aqueous sample solution was acidified with 20 μL of trifluoroacetic acid and derivatized–extracted with 500 μL of hexamethyldisilazane (HMDS) for 10 min. HMDS (upper) phase was analyzed by GC-MS using gas chromatograph Agilent 7890 A and mass selective detector Agilent 5976 C equipped with capillary column HP-5ms, 30 m x 0.25 mm x 0.25 μm under the operation parameters: Inlet temperature: 280 °C, injection volume: 1 μL, injection pulse: 0.2 min at 20 Psi, temperature program: 50 °C – 2 min – 10°C/min – 300°C – 15 min, electron ionization: 70 eV, and mass scan: 29–520 *m*/*z*. Mass spectral library NIST 08 as well as mass spectra and retention times obtained from analysis of standards under identical conditions were used for reliable identification.

Reference

1. E. Petala, K. Dimos, A. Douvalis, T. Bakas, J. Tucek, R. Zbořil and M. A. Karakassides, *J. Hazard. Mater.*, 2013, **261**, 295.

Supporting figures

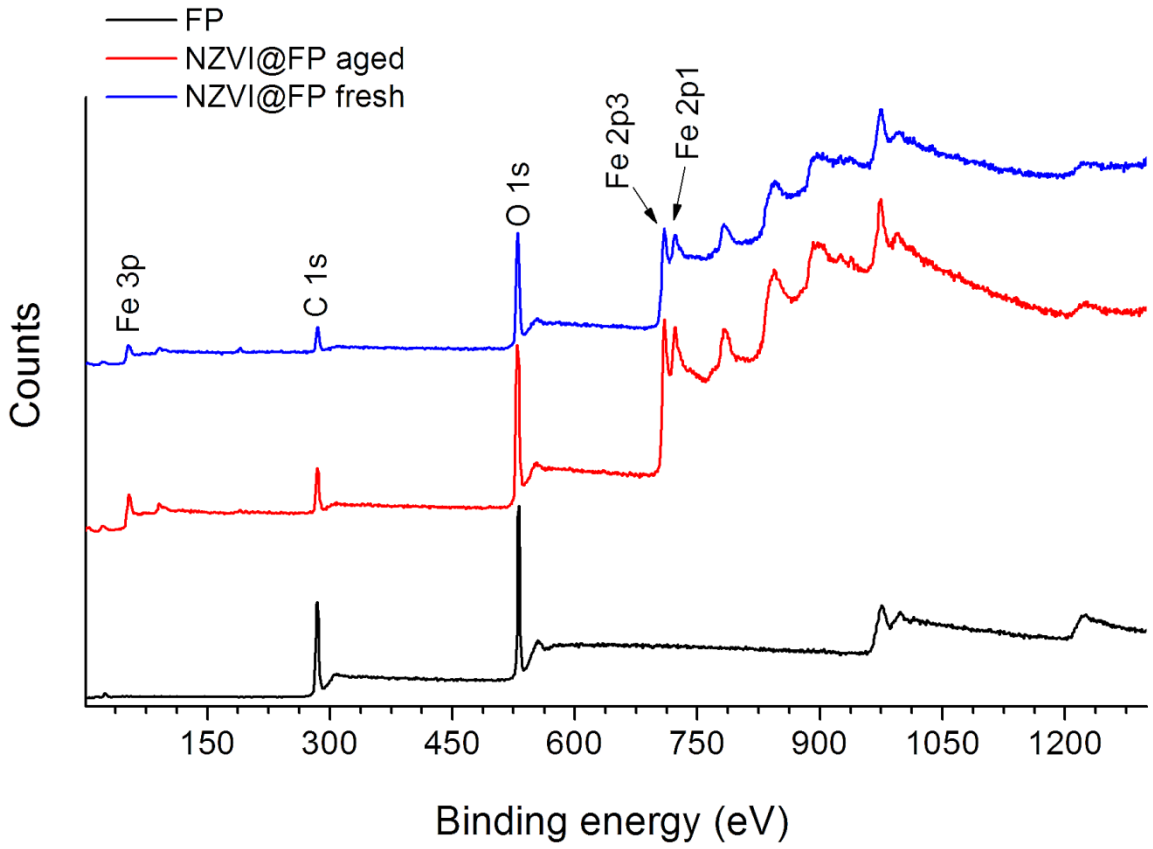

Fig. S1. The recorded XPS spectra of neat filter paper (FP, black), fresh NZVI@FP (blue) and aged NZVI@FP (red) showing the binding energy peaks.

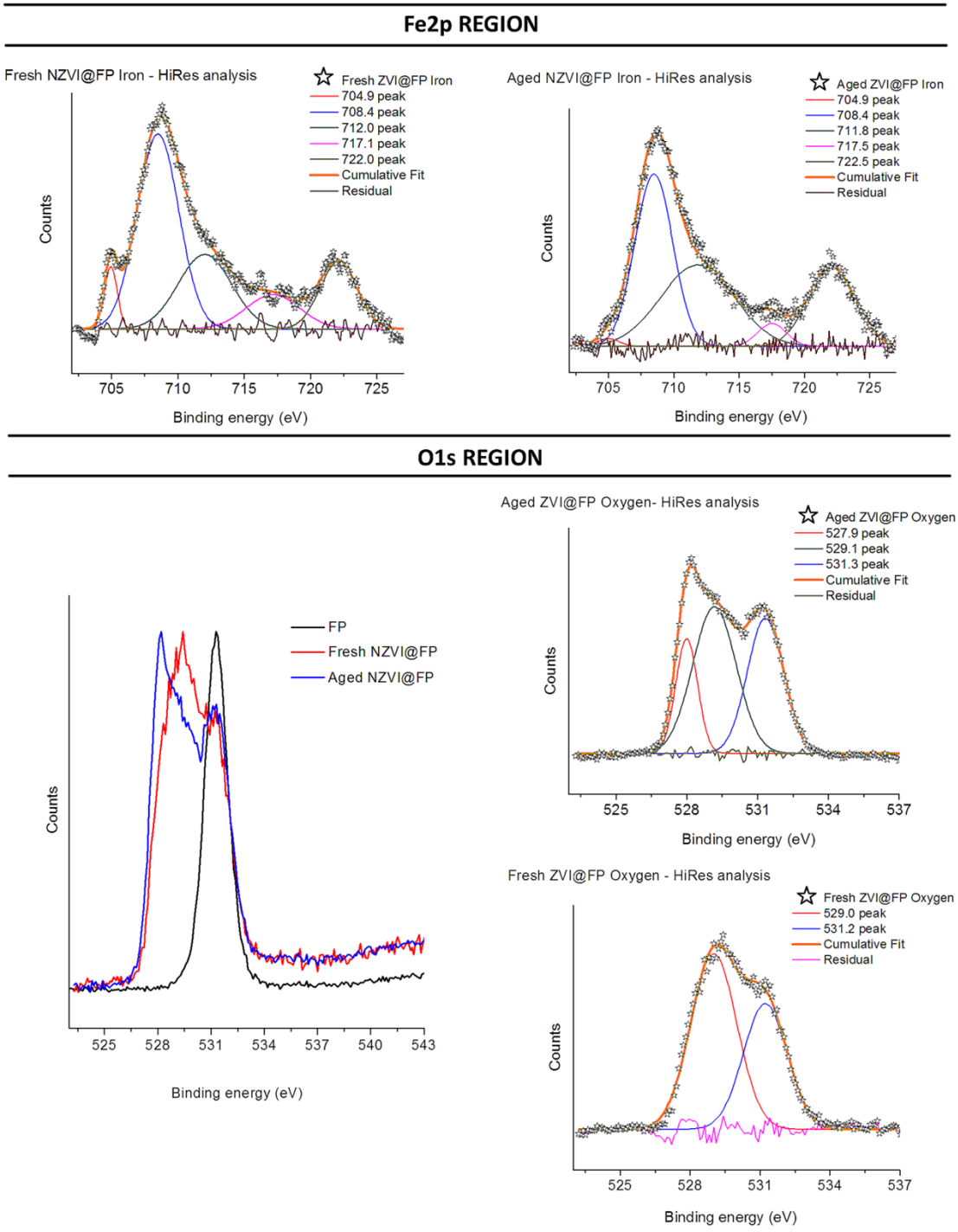

Fig. S2. The high-resolution XPS spectra showing the electronic fingerprints of the neat filter paper (FP), the freshly prepared NZVI@FP and one-month aged NZVI@FP material, recorded in different binding regions (along the Fe2p and O1s absorptions).

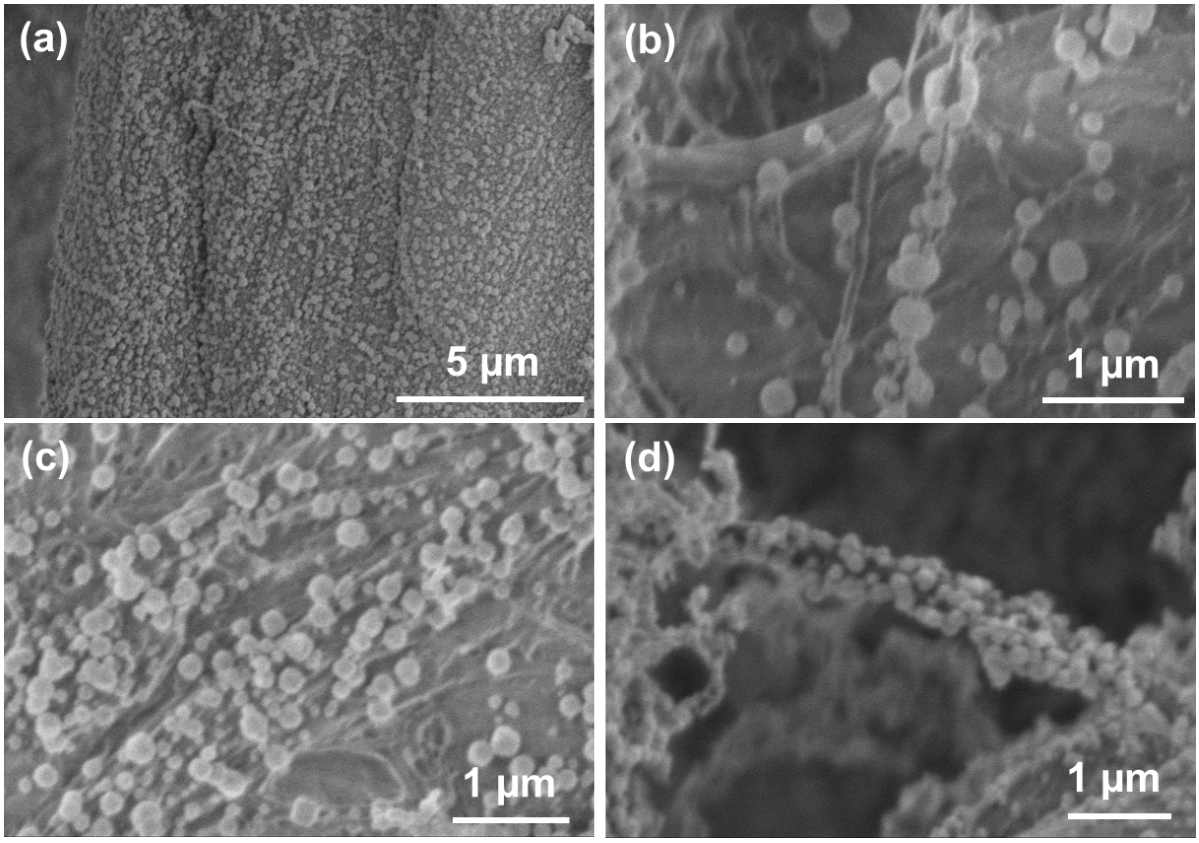

Fig. S3. Scanning electron microscopy (SEM) images of NZVI@FP loaded with 5% in weight of NZVI.

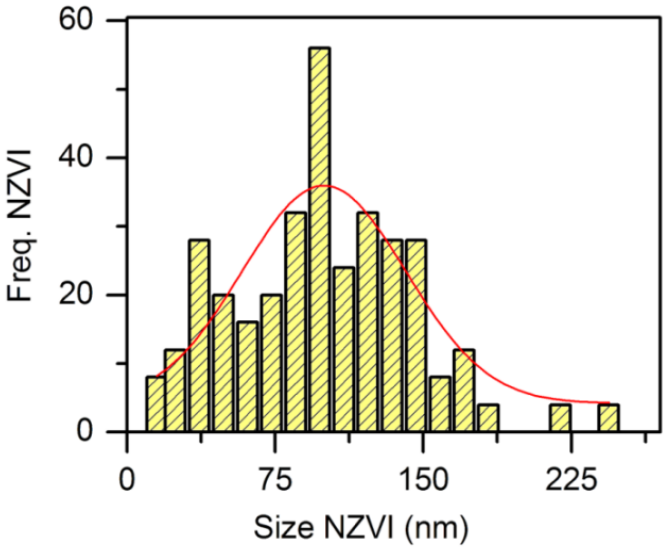

Model: Gaussian distribution analysis
Equation

$$y = y_0 + \frac{A}{w\sqrt{\pi/2}} e^{-2\frac{(x-x_c)^2}{w^2}}$$

	Value		Standard Error
y_0	1.0576		1.55782
x_c	99.65793	(nm)	6.76091
w	82.85822	(nm)	23.01493

Fig. S4. The statistical analysis of the particles size distribution of NZVI@FP as derived from TEM micrograph using a Gaussian distribution function. The derived mean diameter (x_c) for the NZVI was ~100 nm, with Gaussian half-width (w) of ~80 nm.

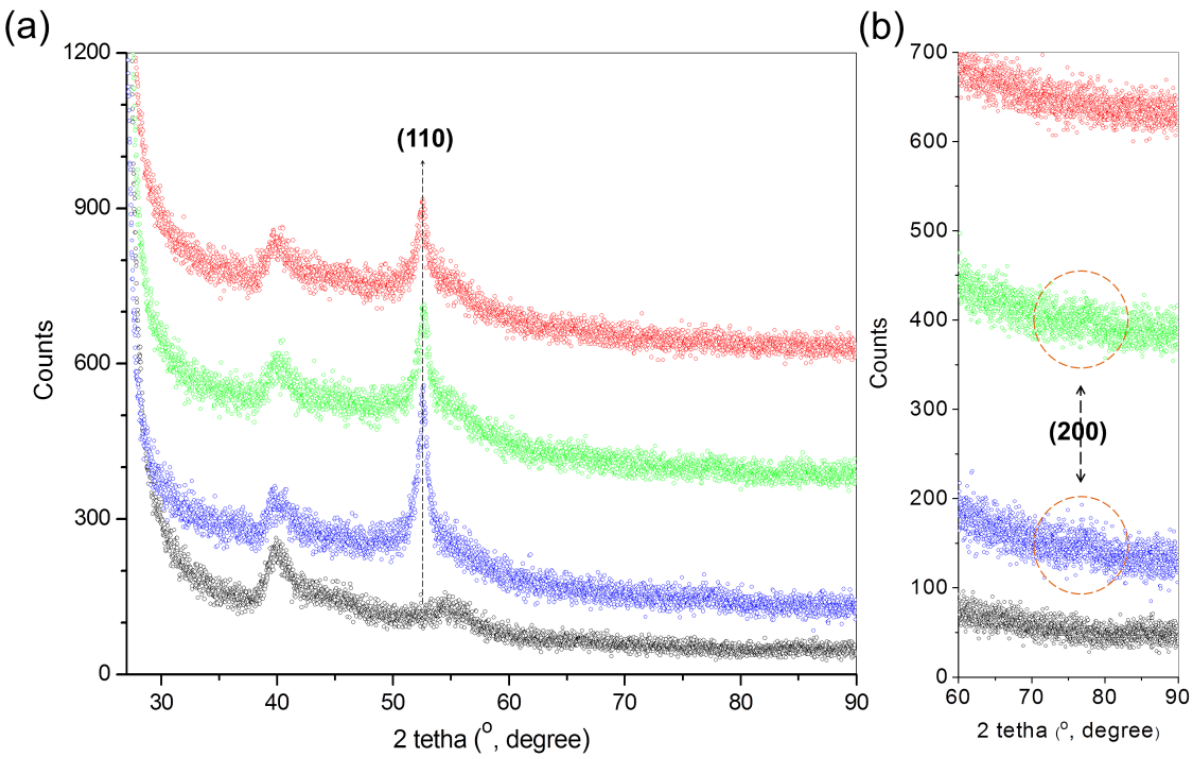

Fig. S5. (a) XRD patterns of FP (black), NZVI@FP (5% of NZVI in weight) (blue), NZVI@FP (4% of NZVI in weight) (green) and NZVI@FP (2.5% of NZVI in weight) (red) showing the peaks corresponding to α-Fe phase. The weight of NZVI is obtained by subtracting weight of FP from the total weight of the composite. Additional note: a broad and very weak peak (200), as shown in panel (b) and highlighted with a circle, can be extracted from the scattering profile for the higher loading of NZVI (4% and 5% wt) at 2θ = 77.3 degrees. This signal is also attributable to the α-Fe phase.

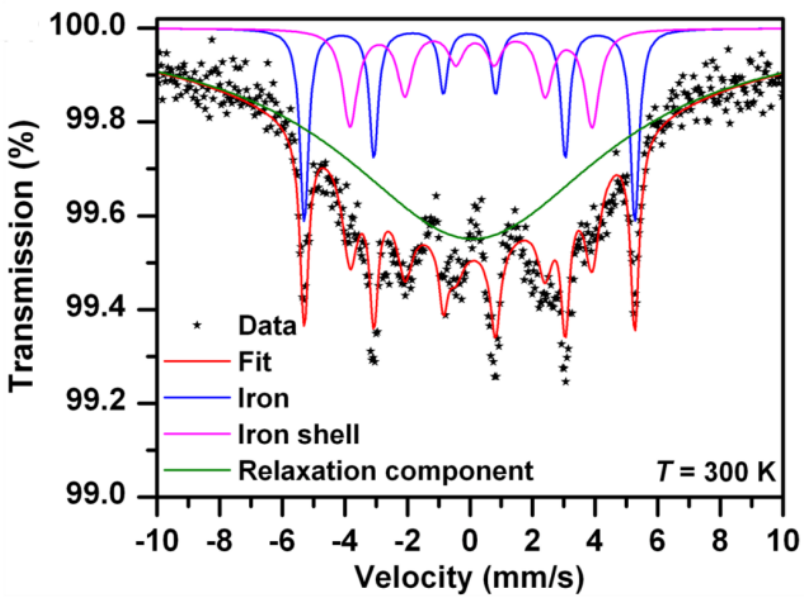

Fig. S6. Zero-field room-temperature ^{57}Fe Mössbauer spectrum of NZVI@FP composite (NZVI loaded as 5% in weight). For more information, see notes on analysis of the room-temperature ^{57}Fe Mössbauer spectrum of NZVI@FP composite reported at page 12.

T (K)	B_{ext} (T)	Component	δ ± 0.01 (mm/s)	ΔE_Q ± 0.01 (mm/s)	B_{hf} ± 0.3 (T)	B_{eff} ± 0.3 (T)	RA ± 1 (%)	Assignment
300	0	Sextet	0.00	0.00	33.0	------	10	Iron
		Sextet	0.10	– 0.13	24.0	------	8	Iron shell
		Singlet	0.10	--------	-----	------	82	Relaxation component
5	5	Sextet	0.11	0.00	-----	28.5	48	Iron
		Sextet	0.22	0.00	-----	19.7*	8	Iron shell
		Doublet	0.23	0.45	-----	------	44	Relaxation component

Table S1. Values of the Mössbauer hyperfine parameters, derived from the fitting of the measured Mössbauer spectra of the NZVI@FP sample at low (T = 5 K, in-field) and high (T = 300 K, no-field) temperature, where T is the temperature, B_{ext} is the external magnetic field, δ is the isomer shift, ΔE_Q is the quadrupole splitting, B_{hf} is the hyperfine magnetic field, B_{eff} is the effective hyperfine magnetic field (i.e., a vector sum of B_{ext} and B_{hf}), and RA is the relative spectra area of individual spectral component. Isomer shift values are related to α-Fe at room temperature. The symbol (*) indicates the average B_{eff} value derived employing the distribution of the effective hyperfine magnetic field.

Analysis of the Mössbauer spectroscopy results obtained at 300 K and in an absence of an external magnetic field. The room-temperature zero-field ^{57}Fe Mössbauer spectroscopy was employed, in addition to the in-field low temperature experiments reported in the main text, in order to dissect further the electronic fingerprints of the Fe in the NZVI@FP sample. The result is shown in Fig. S6 and in Table S1 the Mössbauer parameters obtained at 300 K and 5 K are collected together. The spectrum shown in Fig. S6 displays three spectral components, i.e., the two sextets and one broad singlet. The sextet with the zero isomer shift (δ), zero quadrupole splitting (ΔE_Q) and higher value of the hyperfine magnetic field (B_{hf}) corresponds to the zero-valent iron (blue line in Fig. S6). For the second sextet component with the lower B_{hf}, δ and ΔE_Q values do not resemble those typically reported for zero-valent iron (magenta line, Fig. S6). The non-zero value of ΔE_Q indicates non-spherical distribution of the electronic charge around the Fe probed nucleus. This effect in turn modifies the *s*-electron distribution in the Fe nucleus, altering the monopole interaction and increasing the δ value. Thus, the second sextet can be assigned to the iron atoms occupying the surface layers of the zero-valent iron nanoparticles (in agreement with the low temperature and in-field results). The smaller B_{hf} value compared to that of the first sextet can be explained in terms of definite shell size and weakening of magnetic bonds among iron magnetic moments. The nanoparticle shell is of zero-valent iron chemical nature; however, its structural and magnetic properties slightly differ to those of the core, due to the interaction with the cellulose fibers. The singlet component (green line, Fig. S6) shows the same value of δ and can be also ascribed to the shell of iron nanoparticles. Whereas the sextet reflects well-formed surface nanoparticle shell, the singlet represents a thinner shell, probably not so well developed. More precisely, the singlet is a relaxation component, when iron magnetic moments thermally fluctuates among the easy axis of magnetization, energetically favored by the shell magnetic anisotropy, with the relaxation time (τ) almost identical with the characteristic measuring time (τ_m) of the Mössbauer technique (~10^{-8}). Thus, at room temperature, these nanoparticle shells undergo a superparamagnetic relaxation as demonstrated by magnetization measurements. For well-defined nanoparticle shells, τ is much longer than τ_m, implying that these shells are in a magnetically-blocked state. Therefore, nanoparticles in the NZVI@FP sample exhibit a pseudo core-shell architecture, a core made up of zero-valent iron and a shell of zero-valent iron origin but with altered structural and magnetic features due to interaction with cellulose. The shells show a size distribution, probably as the result of a various degree of attachment of nanoparticles to the cellulose.

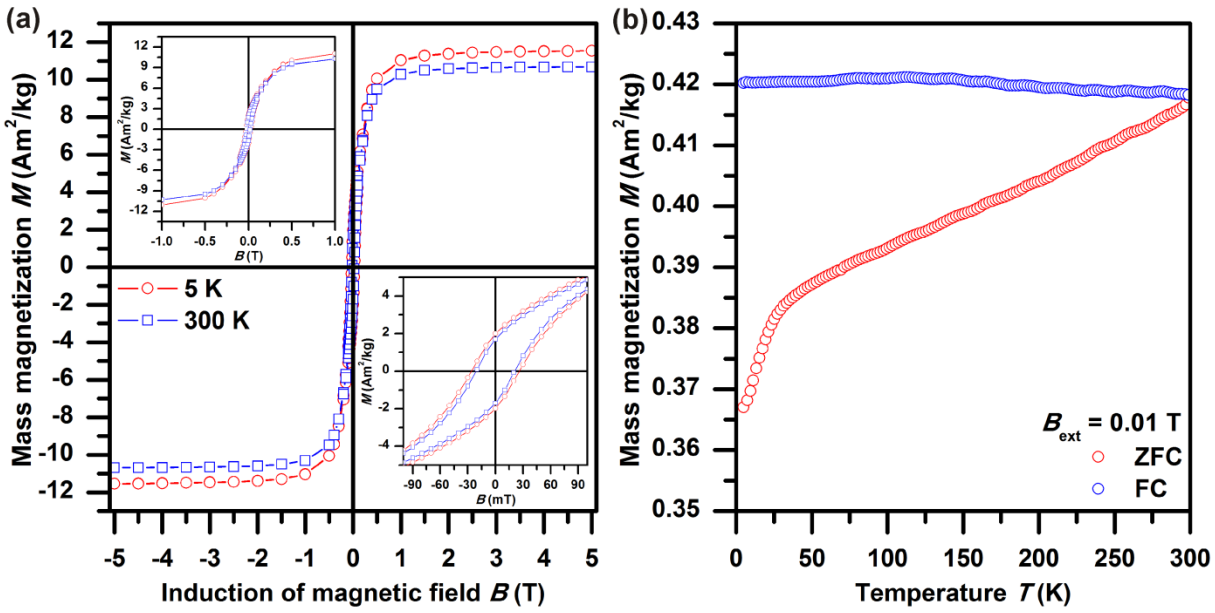

Fig. S7. (a) Hysteresis loops and ZFC/FC magnetization curves of the NZVI@FP composite (5 % of NZVI in weight), measured at 5 K (red circles) and at 300 K (blue squares). (b) Zero-field-cooled and field-cooled magnetization curves of NZVI@FP composite (NZVI load equal to 5% in weight), measured under an external magnetic field, B_{ext}, of 0.01 T.

T (K)	M_{S+} ± 0.01 (Am²/kg)	M_{S-} ± 0.01 (Am²/kg)	B_{C+} ± 0.1 (mT)	B_{C-} ± 0.1 (mT)	M_{R+} ± 0.01 (Am²/kg)	M_{R-} ± 0.01 (Am²/kg)
5	11.54	– 11.54	26.0	– 26.0	1.98	– 1.98
300	10.69	– 10.69	21.0	– 21.0	1.70	– 1.70

Table S2. Parameters of the hysteresis loops of the NZVI@FP sample (5% of NZVI in weight), measured at the temperature of 5 K and 300 K. M_{S+} represents the saturation of magnetization at 5 T, M_{S-} is the saturation magnetization at – 5 T, B_{C+} indicates the positive coercivity, B_{C-} is the negative coercivity, M_{R+} is the positive remanent magnetization and M_{R-} is the negative remanent magnetization.

Scheme S1. Possible mechanism for the hydroxylation of phenol.

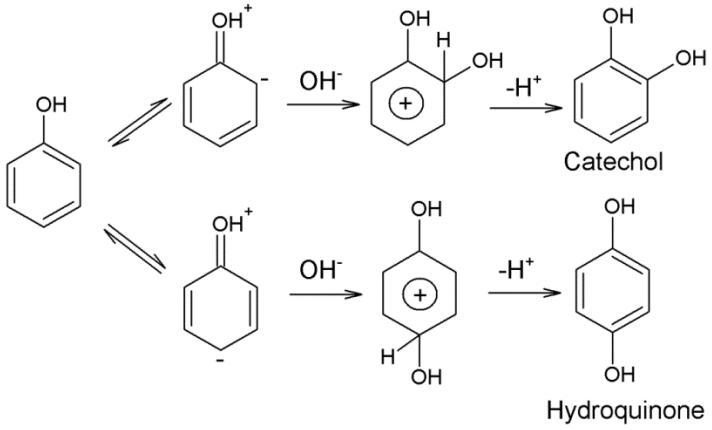

The reaction path in this study involved the primary oxidation of NZVI with H_2O_2 yielding OH· (hydroxyl radical) and OH^- species (Eq. 1 and Eq. 2, see below). The OH· radical attacks the phenol ring, producing catechol, hydroquinone (Scheme 1) and trace amounts of trihydroxybenzene. The hydroxylation of phenol mainly follows a free radical mechanism which is similar to the literature reports[2] using ZVI as a catalyst, i.e.,

$$Fe^0 \rightarrow Fe^{2+} + 2e^- \qquad \text{Eq. (1)}$$

$$Fe^{2+} + H_2O_2 \rightarrow Fe^{3+} + \cdot OH + OH^- \qquad \text{Eq. (2)}$$

References

2. (a) D. H. Bremner, A. E. Burgess, D. Houllemare and K. C. Namkung, *Appl. Catal. B-Environ.*, 2006, **63**, 15; (b) H. Q. Sun, G. L. Zhou, S. Z. Liu, H. M. Ang, M. O. Tade and S. B. Wang, *ACS Appl. Mater. Interfaces*, 2012, **4**, 6235; (c) A. Shimizu, M. Tokumura, K. Nakajima and Y. Kawase, *J. Hazard. Mater.*, 2012, **201**, 60; (d) G. B. O. de la Plata, O. M. Alfano and A. E. Cassano, *J. Photochem. Photobio. A*, 2012, **233**, 53.

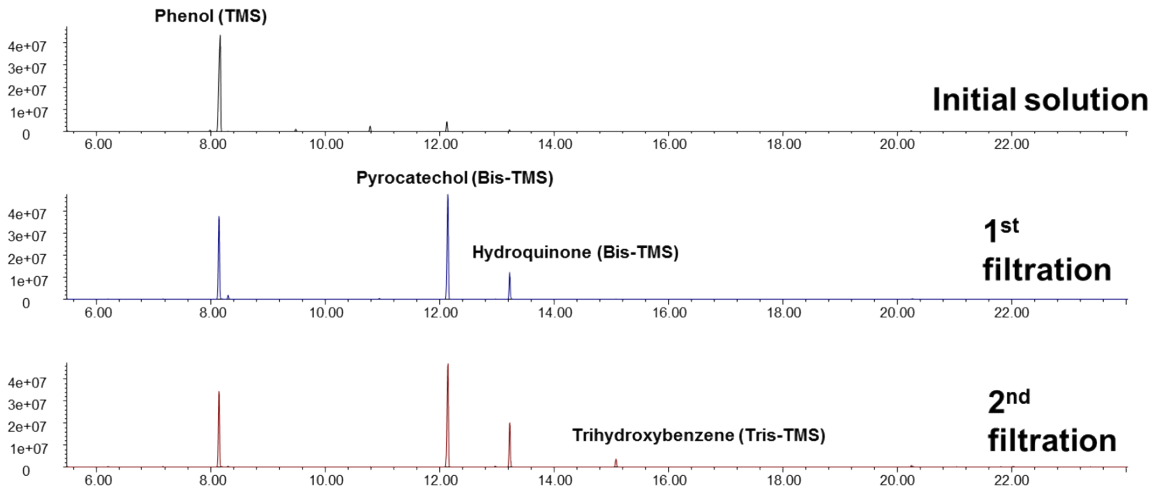

Fig. S8. GC-MS profile of aromatic compounds (after silanization treatment) identified in phenol hydroxylation using NZVI@FP (5 % wt) as membrane catalyst.

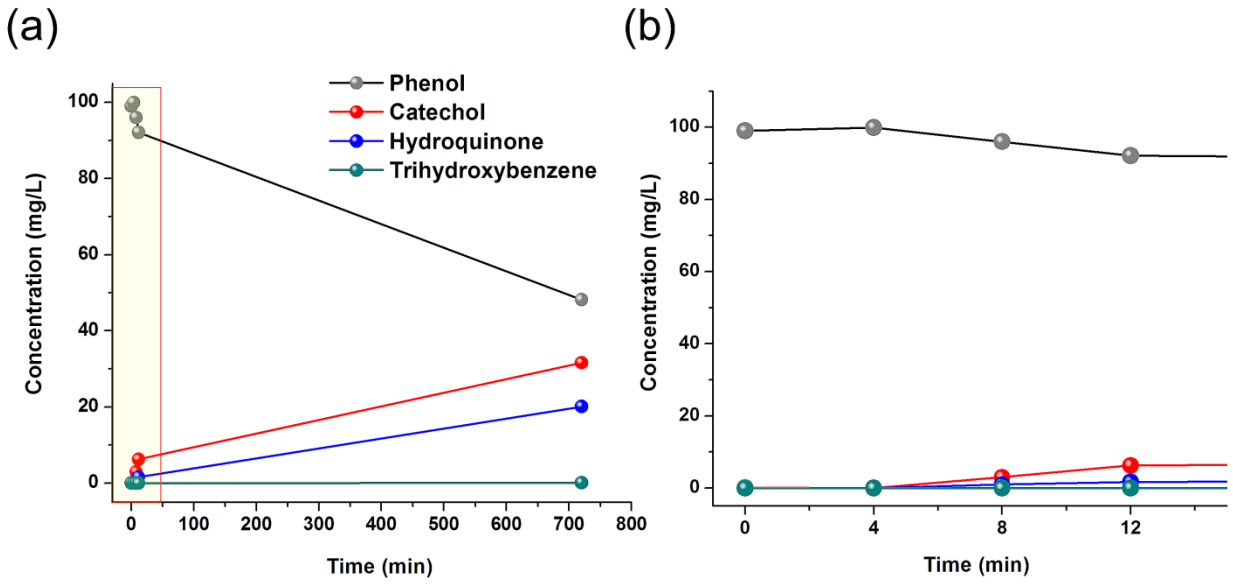

Fig. S9. (a) The formation of the aromatic compounds (catechol, hydroquinone, trihydroxybenzene) identified from control experiments using the synthesized NZVI powder as catalyst. Panel (b) shows the rate of formation of catechol, hydroquinone, trihydroxybenzene in the initial stage of the oxidation reaction (0 min-12 min) from magnification of the data reported in the panel (a) (boxed data).

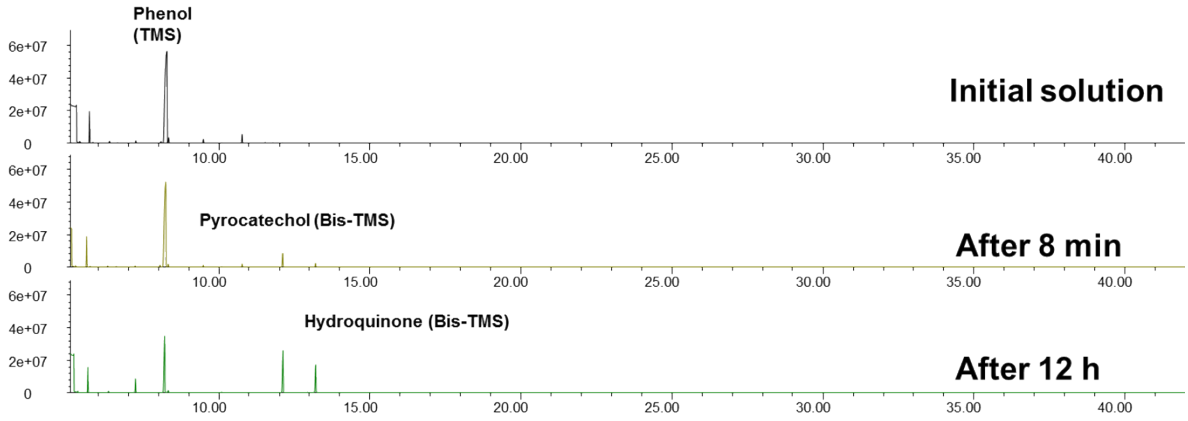

Fig. S10. GC-MS profile of aromatic compounds (after silanization treatment) identified in the control experiment using the as synthesized NZVI powder as catalyst.